SUPPLEMENTARY MATERIALS

Sulfide binding properties of truncated hemoglobins.

Francesco P. Nicoletti, Alessandra Comandini, Alessandra Bonamore, Leonardo Boechi, Fernando Martin Boubeta, Alessandro Feis, Giulietta Smulevich and Alberto Boffi.

Details of the purification procedures of Tf-trHb and its mutants.

Cells (*Escherichia coli* DE3) bearing recombinant Tf-trHb or its mutants were harvested by centrifugation and disrupted by sonication by standard procedures. The supernatant was dyalized against 10 mM phosphate buffer at pH 7.0 at 4 °C for 24 hours and then loaded on a DEAE cellulose column equilibrated with the same buffer. The protein was then eluted with a linear gradient from 0 to 0.5 M NaCl in 50 mM phosphate buffer. The proteins eluted at 0.15 M NaCl and were dyalized again (48 h) in diluted buffer (10 mM phosphate pH 7.0). Thereafter, a hydroxylapatite (Biorad) chromatography was carried out with a linear gradient from 10 to 50 mM phosphate buffer. All proteins eluted at 20 mM phosphate concentration and appeared as a single band on a SDS page. The UV visible spectra of the proteins obtained from the first and second step are reported in Fig. S1. The difference spectrum between the Tf-trHb hemoglobin as obtained in the two purification steps clearly indicate the presence of a sulfide adduct with the typical absorption maximum at 426 nm.

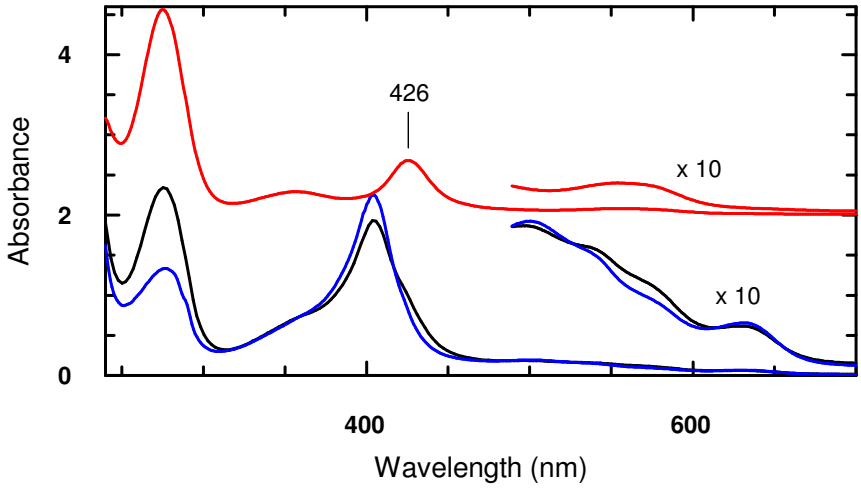

Figure S1. UV-Vis spectra of Tf-trHb at different stages of purification.

The spectra of the protein were taken after the first purification step on a DEAE cellulose (0,15 M phosphate buffer at pH 7.0) (black line). The second spectrum (blue line) was recorded

after the second purification step on a hydroxylapatite column (20 mM phosphate buffer at pH 7.0). The red line is the normalized difference spectrum (blue line *minus* 1.22×(black line)).

UV-visible and resonance Raman spectra of Tf-trHb at two different Na_2S concentration.

The spectra, taken at 0.3 mM and 5 mM Na_2S are compared in order to validate the higher concentration of sulfide used in resonance Raman experiments. The higher concentration were used in order to compensate sulfide loss due to H_2S formation or due to sulfide oxidation during the relatively long exposure of the sulfide containing solution to aerated conditions under laser excitation.

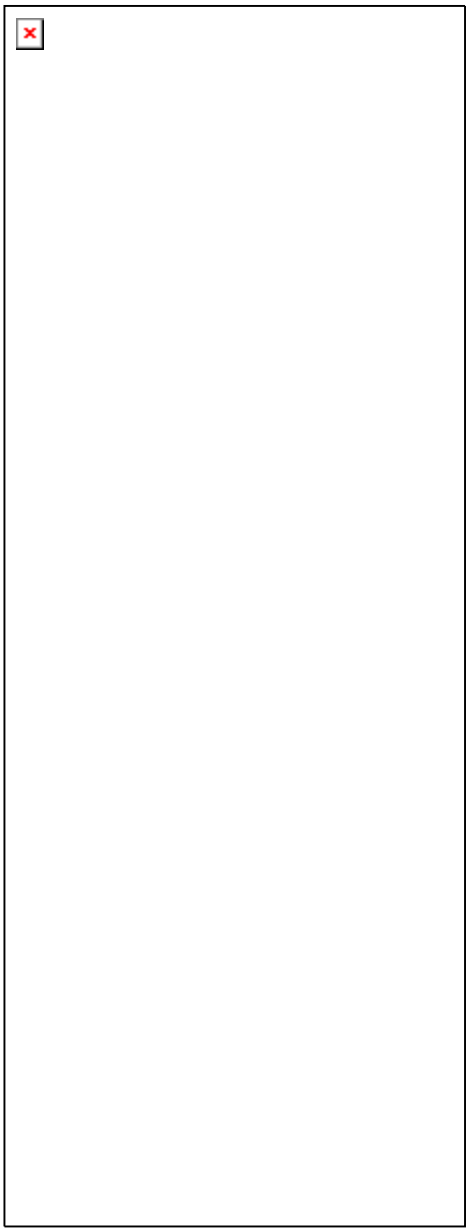

Figure S2. UV-Vis electronic absorption (A) and resonance Raman (A', A") spectra (taken with λ_{exc}: 413.1 nm) of ferric wild type *Thermobifida fusca* (30 μM) at pH 7 in phosphate buffer 100 mM, in the presence of 5 mM (a) and 300 μM (b) of Na_2S solution. A 10-fold excess of ligand has been used according to $K_{(HS-)}$ M^{-1} 2.8×10^6 (see Table 2).

Panel A': High frequency RR spectra: (a), 10 mW laser power at the sample, average of three spectra with 540 s integration time, (b), 3 mW laser power at the sample, average of four spectra with 180 s integration time.

Panel A'': Low frequency RR spectra: (a), 10 mW laser power at the sample, average of two spectra with 1800 s integration time, (b), 3 mW laser power at the sample, average of four spectra with 300 s integration time. The $\upsilon_{(Fe-S)}$ stretching frequency is indicated in bold.

UV-Visible and RR spectra of single point mutants WG8F-trHb and YCD1F-trHb.

Upon ligand binding, the UV-Vis spectra are similar to those of wild type Tf-trHb, its the triple mutant YB10F-YCD1F-WG8F (3F-Tf-trHb) and Bs-trHb, showing bands at 426, 550, and 575(sh) nm. Accordingly, the resonance Raman spectra (Fig. 2S, panels A', B') of the sulfide complexes displayed typical ferric, low-spin iron features with ν_3 at 1502-1504 cm^{-1}, ν_2 at 1585 cm^{-1}, and ν_{10} at 1636-1638 cm^{-1}. In the low frequency region (Fig. 2S, panels A", B"), the propionyl bending vibrations [$\delta(C_\beta C_c C_d)$] at 383-384 cm^{-1}, up-shift by 6-7 cm^{-1} upon sulfide binding, as observed for the wild type Tf-trHb and its triple mutant and Bs-trHb. In all the samples the ν(Fe–S) stretching mode is assigned to the strong band around 375 cm^{-1}. The low expression level of YB10F- Tf-trHb did not allow sufficient amount of sample for a full RR characterization.

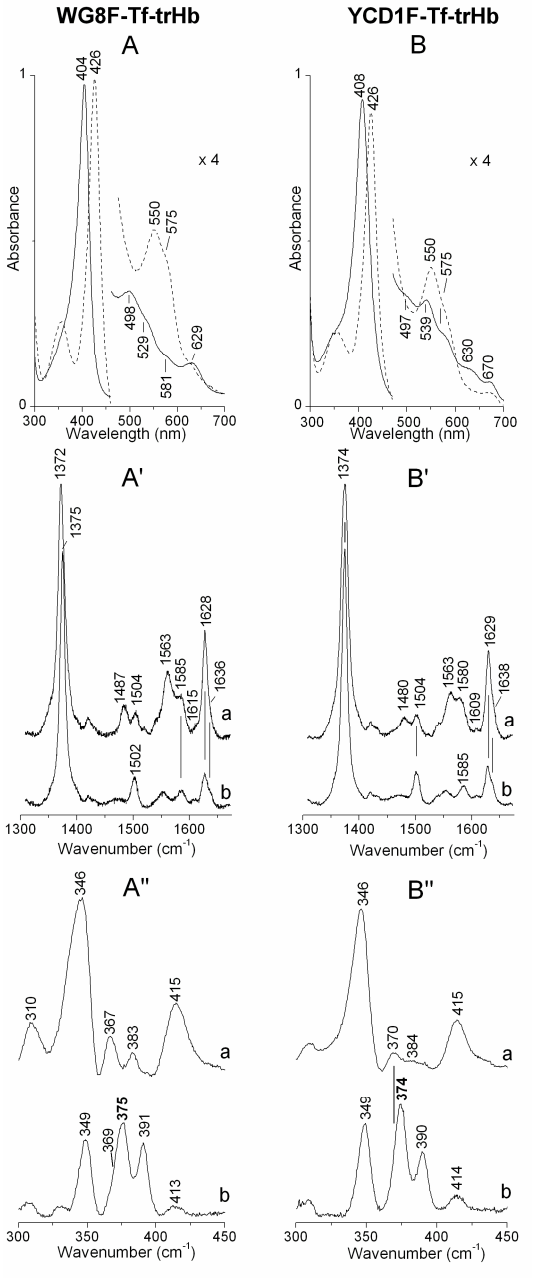

Figure S3. UV-vis electronic absorption and resonance Raman spectra of WG8F Tf-trHb and YCD1 Tf-trHb at pH 7 in phosphate buffer 100 mM. **Panels A,B:** UV-vis electronic absorption spectra of WG8F Tf-trHb (A) and YCD1 Tf-trHb (B) in the absence (solid lines) and in the presence (dashed lines) of 5mM Na_2S. **Panels A',B':** High frequency RR spectra of WG8F-Tf-trHb (A'), YCD1-Tf-trHb (B'), in the absence (traces a) and in the presence (traces b) of 5mM Na_2S, taken with λ_{exc}: 413.1 nm, 12 mW laser power at the sample, average of four spectra with 150 s integration time. **Panels A",B":** Low frequency RR spectra of WG8F-Tf-trHb (A"), YCD1-Tf-trHb (B"), in the absence (traces a) and in the presence (traces b) of 5mM Na_2S, 12 mW laser power at the sample, average of eight spectra with 300 s integration time. Protein concentrations were in the range of 20-30 μM. The $\upsilon_{(Fe-S)}$ is indicated in bold.

Azide binding and dissociation kinetics.

Azide ligand binding and release kinetic constants were determined in order to validate the use of azide ion as a ligand for displacement reaction with sulfide. Azide is a popular ligand for equilibrium displacement reactions in hemeproteins due to its relatively fast combination and release constants. As shown below, this is the case also for Bs-trHb, Tf-trHb and its mutants.

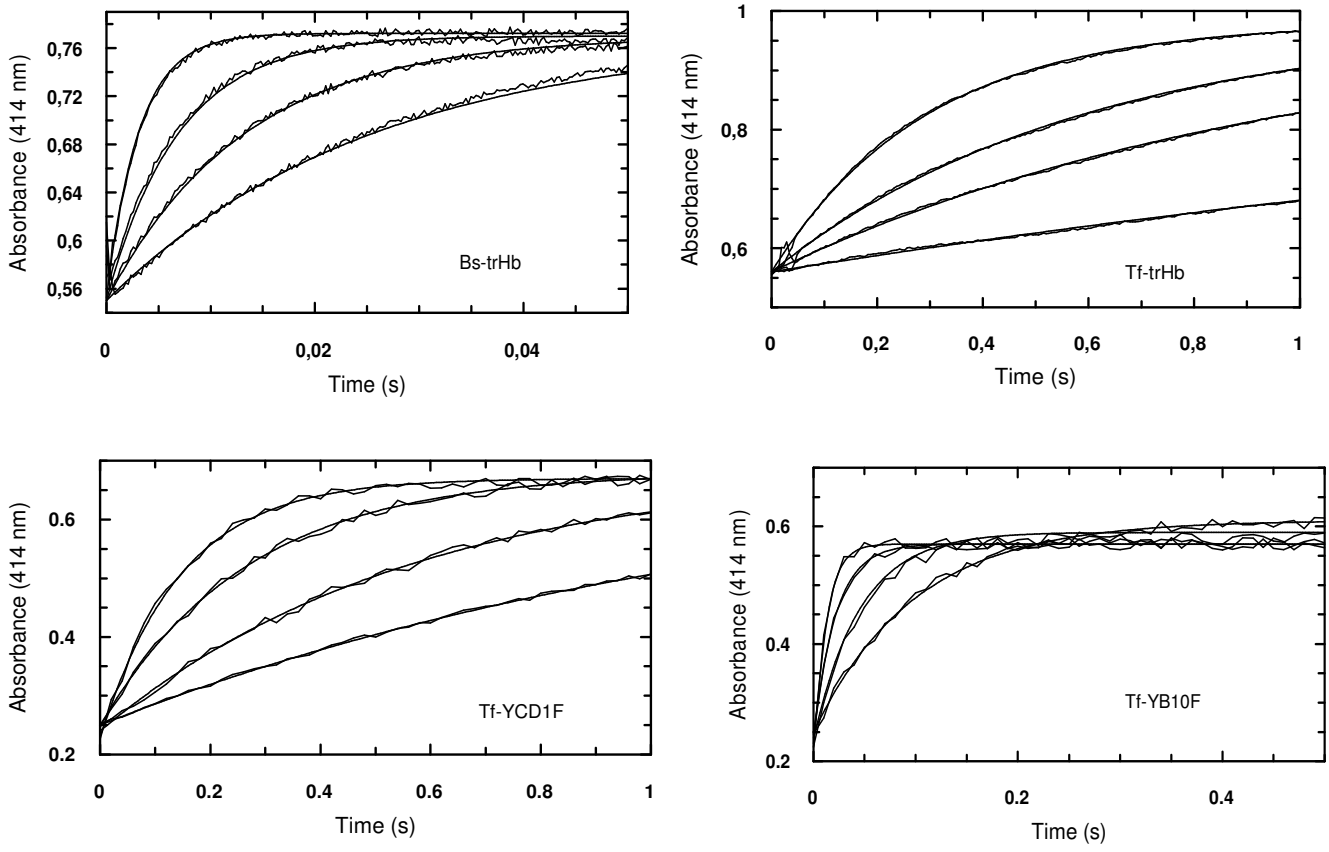

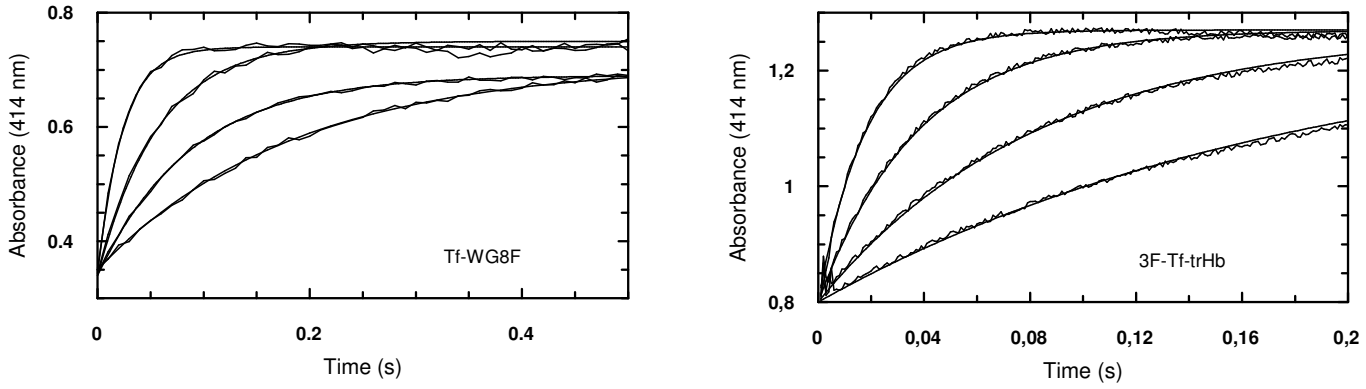

Figure S4. Azide binding kinetics. Azide binding kinetics were carried out by mixing the hemoglobin solutions (Bs-trHb, 6.2 μM; Tf-trHb, 7 μM; 3F-Tf-trHb, 9.5 μM; YB10F-Tf-trHb, 6.5 μM; YCD1F-Tf-trHb, 5.7 μM; YG8F-Tf-trHb, 6.3 μM) with increasing azide concentrations (from top to bottom, 1 mM, 0.5 mM, 0.025 mM and 0.125 mM), in 0.1 M phosphate buffer at pH 7.0 and 25 °C. Each curve was fitted to a single exponential with the standard software provided by Applied Photophysics. Second order plot yielded k_{N3}- values of $2.9 \pm 0.22\times10^{5}$ $M^{-1}s^{-1}$ for Bs-trHb; for $3.4 \pm 0.2\times10^{3}$ $M^{-1}s^{-1}$ Tf-trHb, $5.5 \pm 0.4\times10^{4}$ $M^{-1}s^{-1}$ for 3F-Tf-trHb, $6.8 \pm 0.64\times10^{3}$ $M^{-1}s^{-1}$ for YCD1F-Tf-trHb, $8.4 \pm 0.6\times10^{4}$ $M^{-1}s^{-1}$ for YB10F-Tf-trHb, $3.9 \pm 0.52\times10^{4}$ $M^{-1}s^{-1}$ for WG8F-Tf-trHb.

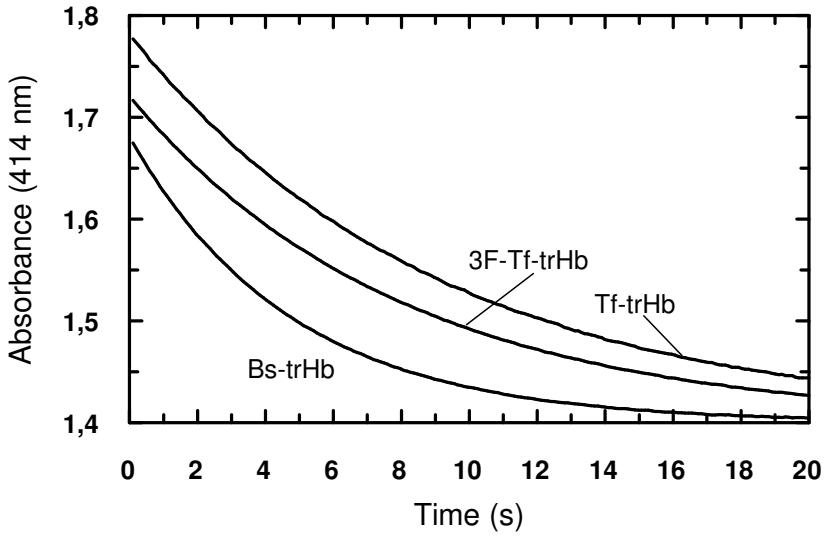

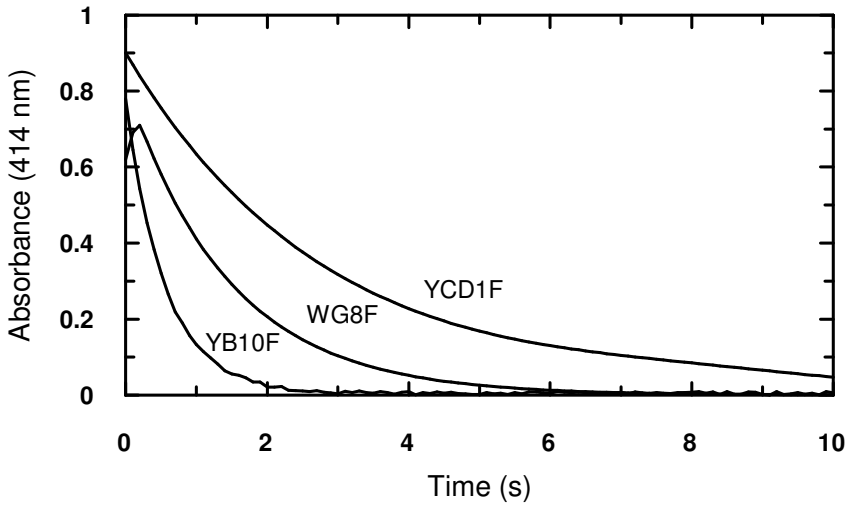

Figure S5. Azide dissociation kinetics. Proteins were saturated with 10 mM sodium azide and mixed with 1 mM sodium sulfide solutions in a stopped flow apparatus. The signal decrease at 414 nm (the peak of the azide adduct) is a first order process corresponding to azide release. Control experiments at 425 nm (not shown) reveal a rise in absorbance with identical time course. Experiments were carried out in 0.1 M phosphate buffer at pH 7.0 and 25 °C. First order rates rates were 0.21± 0.03 s^{-1} for Bs-trHb; 0.11± 0.02 s^{-1} for Tf-trHb; 0.125 ± 0.020 s^{-1} for 3F-Tf-trHb; 0.35 ± 0.03 s^{-1} for YCD1F-Tf-trHb; 1.8 ± 0.05 s^{-1} for YB10F-Tf-trHb; 0.69± 0.02 s^{-1} for WG8F-Tf-trHb.

Azide-sulfide equilibrium displacement titrations.

Equilibrium displacement experiments were carried out in order to double check the values of the thermodynamics constants obtained from the ratio of the measured rates of sulfide combination and sulfide release. Azide thermodynamic binding constants were obtained from the ratio of the kinetic binding constants measured as detailed before. Thus, convenient azide and sulfide concentrations were planned for a full ligand displacement protocol (see legend). The agreement between the values obtained from the kinetic experiments and the equilibrium displacement ones is within the reported experimental error.

Bs-trHb

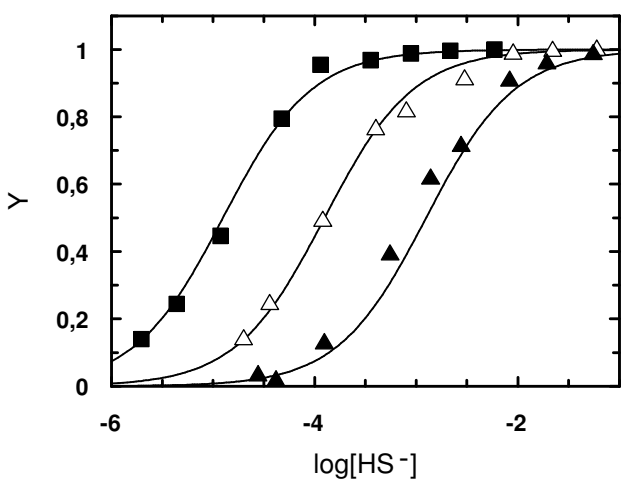

Tf-trHb

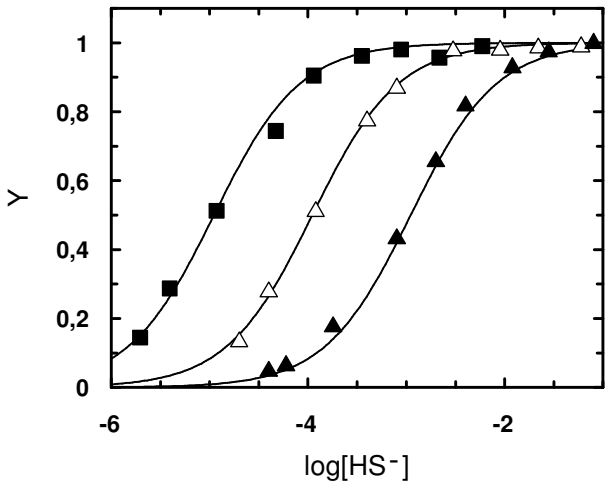

3F-Tf-trHb

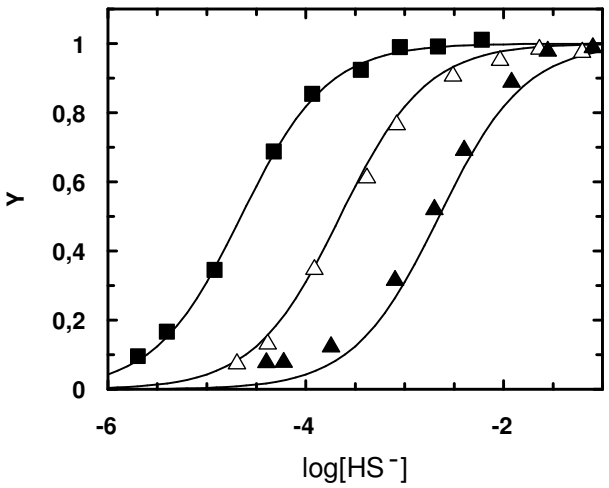

YCD1F-Tf-trHb

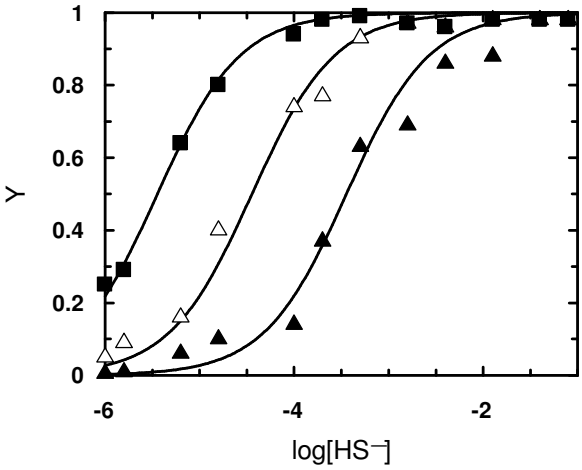

YB10F-Tf-trHb

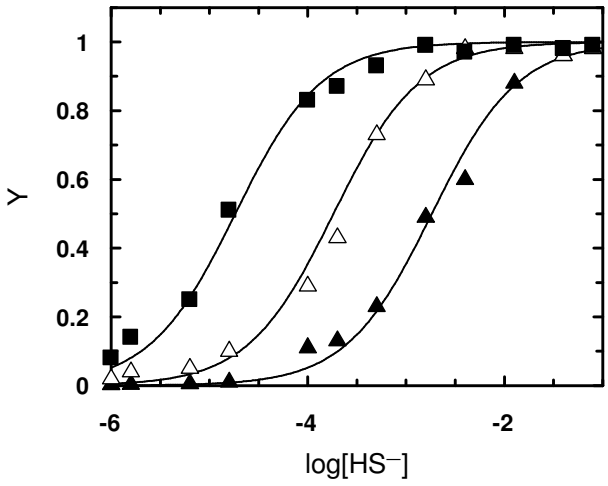

WG8F-Tf-trHb

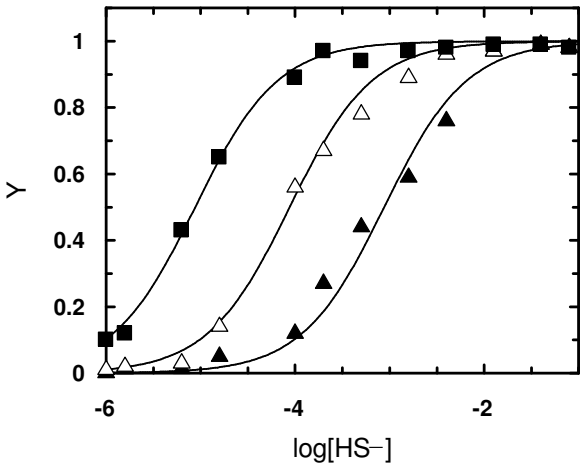

Figure S5. Azide-sulfide equilibrium displacement titrations. Protein solutions (3 ml, 10-12 μM) containing 1 mM (black triangles), 0.1 mM (white triangles) or 0.01 mM (black squares) sodium azide in 0.1 M phosphate buffer at pH 7.0 were placed in a 1 cm quartz cuvette in a HP 8453 diode array spectrophotometer equipped with magnetic stirring and a Peltier thermostatted cell holder. A few μl of a sodium sulfide nonahydrate stock solutions (10 mM or 0.1 mM) were added and the absorption spectrum was recorded after 5 minutes. Absorbance changes were transformed into fractional saturation by standard procedures. Experimental data sets relative to each protein were fitted simultaneously to simple ligand binding curves (see also Materials and methods) by a least squares fitting method based on the Matlab program (South Natick, MA, USA). Averaged values of the thermodynamic constants for azide, as estimated from kinetic measurements were used. The following sulfide binding contants k_{HS}- were obtained: $5.0 \pm 0.52\times10^{6}$ M^{-1} for Bs-trHb; $2.8 \pm 0.42\times10^{6}$ M^{-1} for Tf-trHb; $2.0 \pm 0.4\times10^{7}$ $M^{-1}s^{-1}$ for 3F-Tf-trHb; $5.8 \pm 0.64\times10^{6}$ M^{-1} for YCD1F-Tf-trHb; $3.1 \pm 0.6\times10^{7}$ M^{-1} for YB10F-Tf-trHb; $1.13 \pm 0.62\times10^{5}$ M^{-1} for WG8F-Tf-trHb.

Sulfide binding and dissociation kinetics

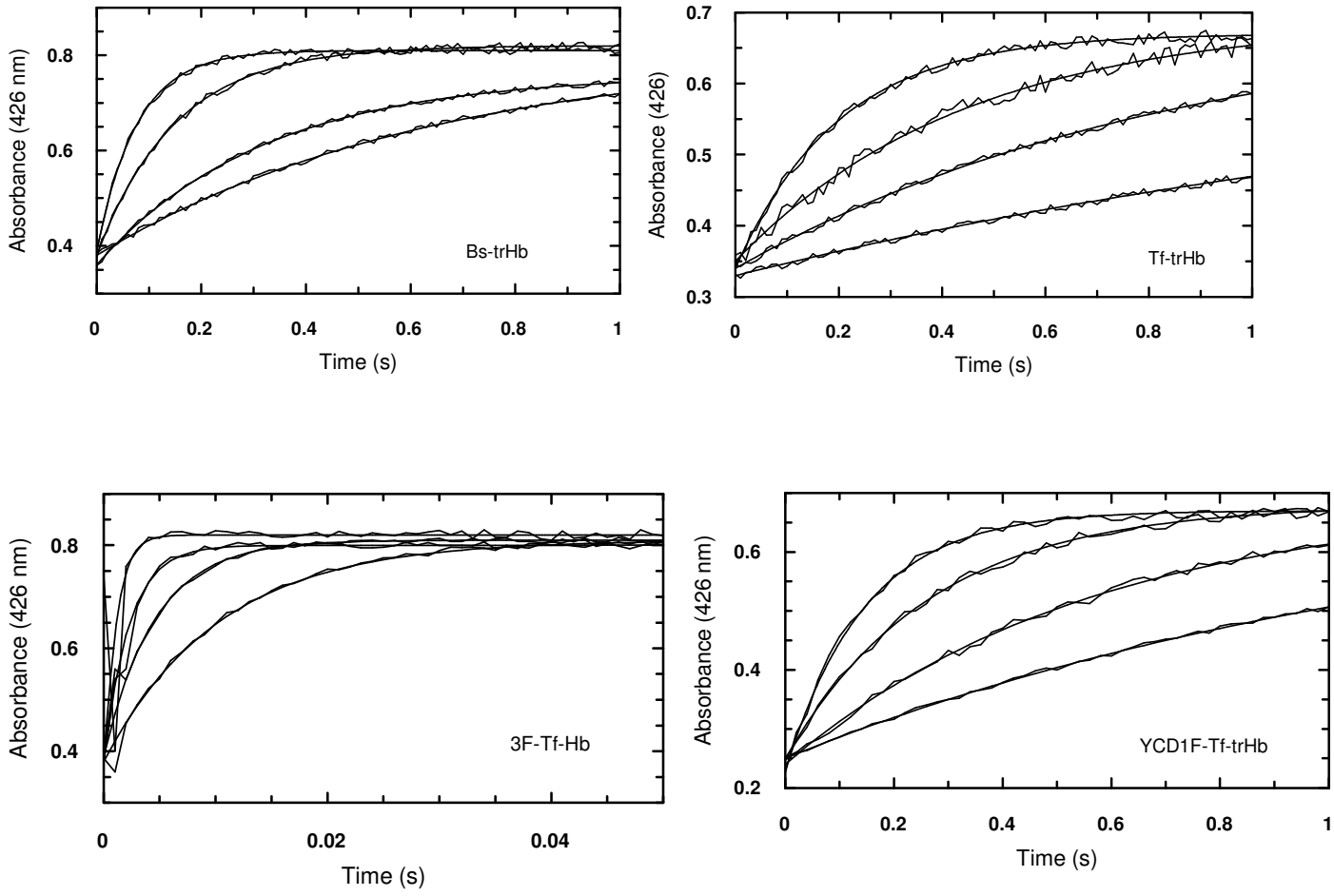

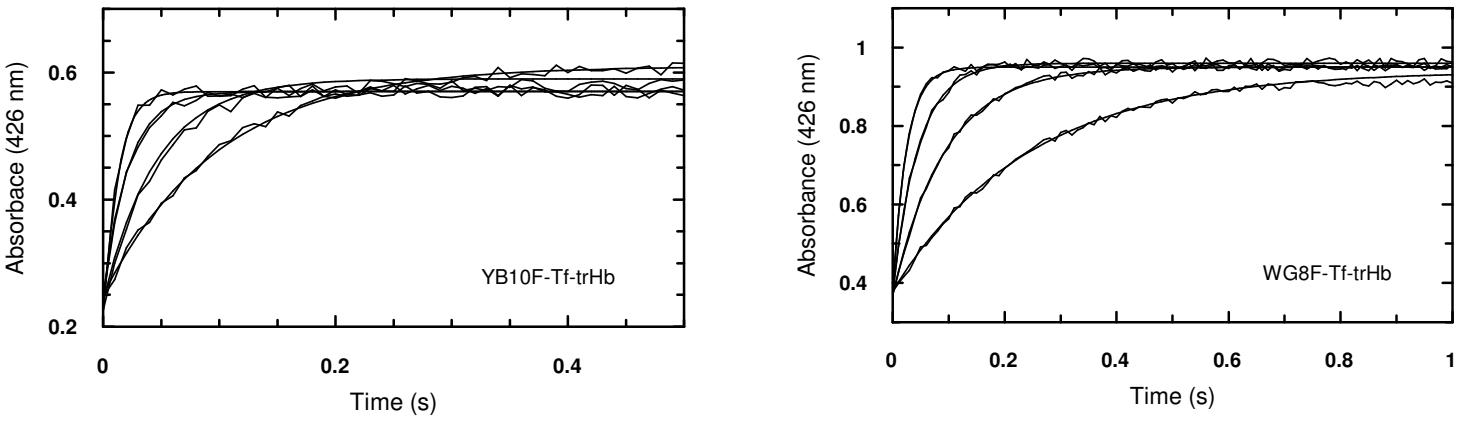

Figure S6. Sulfide combination reactions. Sulfide binding kinetics were carried out by mixing the hemoglobin solutions (Bs-trHb, 6.8 mM; Tf-trHb, 5.8 mM; 3F-Tf-trHb, 7.5 mM; YB10F-Tf-trHb, 4.8 μM; YCD1F-Tf-trHb 5.7 μM; WG8F-Tf-trHb, 8.3 μM) with increasing sulfide concentrations (from top to bottom, 1 mM, 0.5 mM, 0.025 mM and 0.125 mM except in the case of 3FTf-trHb in which the solutions were diluted fourfold), in 0.1 M phosphate buffer at pH 7.0 and 25 °C. Each curve was fitted to a single exponential with the standard software provided by Applied Photophysics. Second order rates rates were $1.3 \pm 0.12\times10^{4}$ $M^{-1}s^{-1}$ for Bs-trHb; for $5.0 \pm 0.21\times10^{3}$ $M^{-1}s^{-1}$ Tf-trHb, $4.4 \pm 0.4\times10^{6}$ $M^{-1}s^{-1}$ for 3F-Tf-trHb, $5.8 \pm 0.34\times10^{3}$ $M^{-1}s^{-1}$ for YCD1F-Tf-trHb; $7.8 \pm 0.6\times10^{3}$ $M^{-1}s^{-1}$ for YB10F-Tf-trHb, $4.1 \pm 0.32\times10^{4}$ $M^{-1}s^{-1}$ for WG8F-Tf-trHb.

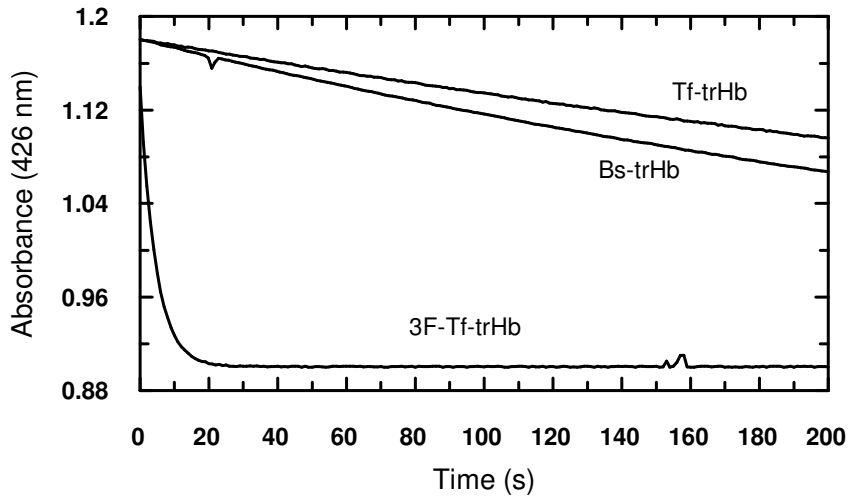

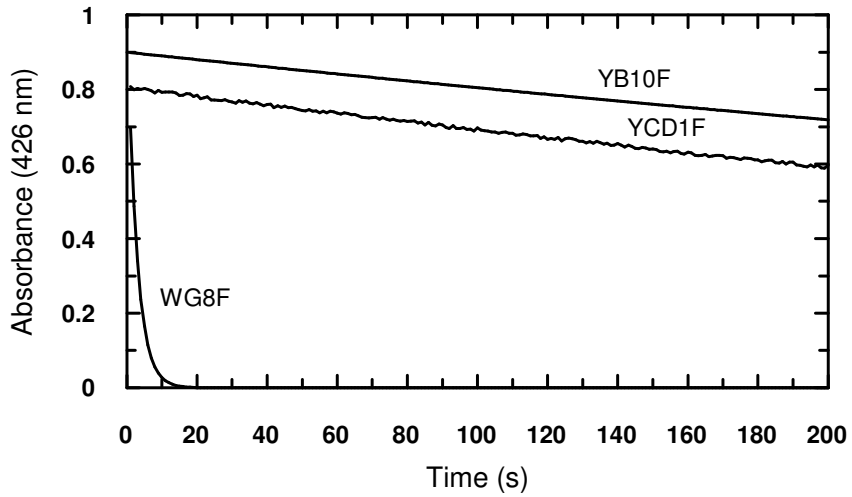

Figure S7. Sulfide dissociation reactions. Kinetics of sulfide release were carried out on proteins (11 mM) saturated with 100 mM sodium sulfide and mixed manually with 100 mM sodium azide solutions in a spectrophotometer. The signal decrease at 425 nm (the peak of the sulfide adduct) is a first order process corresponding to sulfide release. Control experiments at 414 nm (not shown) reveal a rise in absorbance with identical time course. Experiments were carried out in 0.1 M phosphate buffer at pH 7.0 and 25 °C. First order rates rates were $2.6 \pm 0.3\times10^{-3}$ s^{-1} for Bs-trHb; $1.8 \pm 0.2\times10^{-3}$ s^{-1} for Tf-trHb; 0.22 ± 0.02 s^{-1} for 3F-Tf-trHb; $1.0\times10^{-3} \pm 0.1$ s^{-1} for YCD1F-Tf-trHb; $1.2 \pm 0.15\times10^{-3}$ s^{-1} for YB10F-Tf-trHb; 0.36 ± 0.03 s^{-1} for WG8F-Tf-trHb.

Molecular dynamics supplemental information

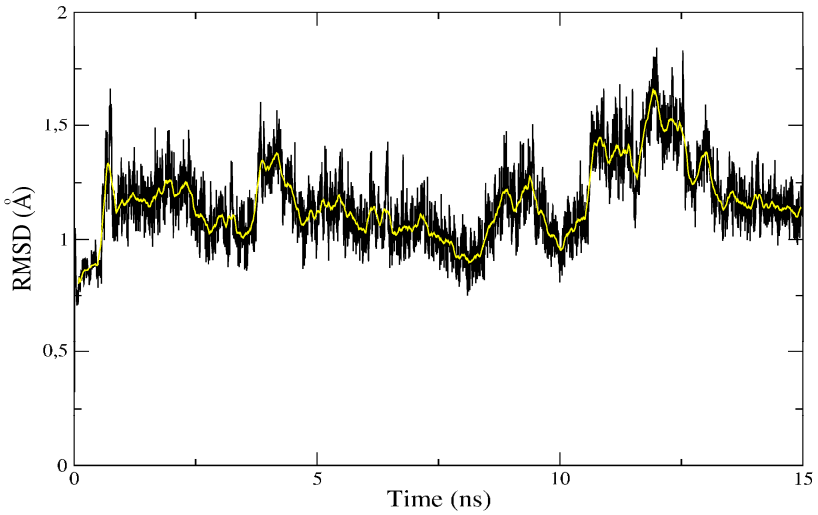

Figure S6. RMSD (backbone) vs time of MD simulation in Tf-trHb-SH^- .

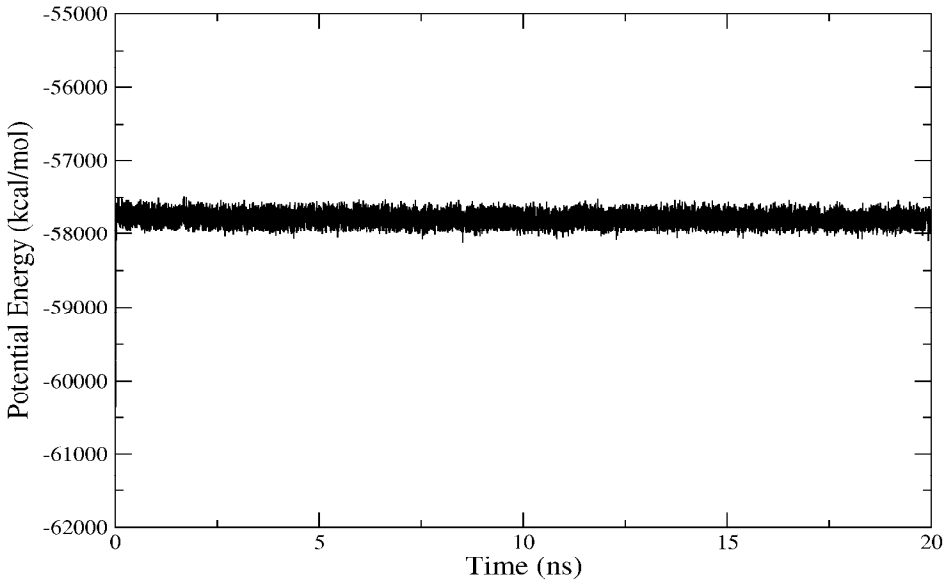

Figure S7. Potential energy vs time of MD simulation in Tf-trHb-SH$^-$.